Indian Journal of Pure & Applied Physics
Vol. 56, February 2018, pp. 108-118

Vibrational spectroscopic investigations, DFT computations, nonlinear optical and other molecular properties of 3-bromo-5-fluorobenzonitrile

S Jeyavijayan[a]*, E Gobinath[a], K Viswanathan[a] & J Senthil Kumar[b]

[a]Department of Physics, Kalasalingam University, Anand Nagar, Krishnankoil 626 126, India
[b]P G & Research Department of Physics, Periyar EVR College, Tiruchirappalli 620 023, India

Received 8 September 2016; accepted 30 October 2017

The FTIR and FT-Raman spectra of 3-bromo-5-fluorobenzonitrile (BFBN) have been recorded in the regions 4000-400 cm^{-1} and 3500-400 cm^{-1}, respectively. Utilizing the observed FT-Raman and FTIR data, a complete vibrational assignment and analysis of the fundamental modes of the compound have been carried out and subsequently confirmed by total energy distribution (TEDs). In the calculations performed to determine the optimum molecular geometry, harmonic vibrational frequencies, infrared intensities and Raman scattering activities, the density functional theory (DFT/B3LYP) method with 6-31+G(d,p) and 6-311++G(d,p) basis sets has been used. The results have been compared with the experimental values. The difference between the observed and scaled wavenumber values of most of the vibrational modes is very small. The NLO properties such as polarizability and first hyperpolarizability of the molecule have been calculated. The effects of frontier orbitals, HOMO and LUMO and the transition of electron density transfer have been discussed. The UV-Vis spectrum has been done which confirms the charge transfer of BFBN. The chemical interpretation of hyperconjugative interactions and charge delocalization has been analyzed using natural bond orbital (NBO) analysis.

Keywords: FTIR, FT-Raman, DFT, 3-bromo-5-fluorobenzonitrile, NLO, NBO

1 Introduction

Benzonitrile and its derivatives have been extensively used in chemistry as a solvent and as a chemical intermediate for the synthesis of pharmaceuticals, dyestuffs and several other important applications[1]. From the spectroscopic point of view, in recent years numerous experimental and theoretical studies have been made on the vibrational spectra of benzonitrile, its mono- and di- substituted derivatives[2,3]. More recently, the FTIR and FT-Raman spectra, MEP and HOMO–LUMO of 2,5-dichlorobenzonitrile have been studied by Palafox *et al.*[4]. However, the detailed B3LYP comparative studies on the complete FTIR and FT-Raman spectra of 3-bromo-5-fluorobenzonitrile (BFBN) have not been reported so far. Further, among DFT calculations, Becke's three parameter hybrids functional combined with the Lee-Yang-Parr correlation functional (B3LYP) is the best predicting results for molecular geometry and vibrational wavenumbers for moderately larger molecules[5]. Hence, in the present investigation, molecular geometry, optimized parameters and vibrational frequencies are computed and the performance of the computational method for B3LYP with the standard 6-31+G(d,p) and 6-311++G(d,p) basis sets are compared. These methods predict relatively accurate molecular structure and vibrational spectra with moderate computational effort.

2 Experimental Details

The compound under investigation namely BFBN was purchased from Lancaster Chemical Company, UK which is of spectroscopic grade and hence used for recording the spectra as such without any further purification. The FTIR spectrum of the compound were recorded in the range of 4000–400 cm^{-1} using a BRUKER IFS-66V FTIR spectrometer equipped with an MCT detector, a KBr beam splitter and a globar source. The spectral resolution is ±1 cm^{-1}. The FT-Raman spectrum of the title compound have been recorded in the Stokes region (3500–400 cm^{-1}) on a computer interfaced BRUKER IFS model interferometer equipped with FRA-106 FT-Raman accessory using Nd: YAG laser source operating at 1.064 nm excitation wavelength, line width with 200 mW power. The frequencies of all sharp bands are accurate to ±1cm^{-1}.

*Corresponding author (E-mail: sjeyavijayan@gmail.com)

3 DFT Calculations

Quantum chemical density functional calculations were carried out for BFBN with the 2009 Window version of the GAUSSIAN suite program[6] using Becke-3-Lee-Yang-Parr (B3LYP) functional[7,8] supplemented with the standard 6-31+G(d,p) and 6-311++G(d,p) basis sets. All the parameters were allowed to relax and all the calculations converged to an optimized geometry which corresponds to a true energy minimum, as revealed by the lack of imaginary values in the wavenumber calculations. The Cartesian representation of the theoretical force constants have been computed at the fully optimized geometry by assuming the molecule belongs to C_s point group symmetry. The transformation of force field from Cartesian to internal local-symmetry coordinates, the scaling and calculation of total energy distribution (TED) were done on a PC with the version V7.0-G77 of the MOLVIB program written by Sundius[9].

4 Results and Discussion

4.1 Molecular geometry

The molecular structure of BFBN is shown in Fig. 1. The title molecule contains bromine, fluorine atoms and C-N group attached with the benzene ring. The experimental and calculated FTIR and FT-Raman spectra of BFBN are given in Figs 2 and 3, respectively. The comparative optimized structural parameters such as bond lengths and bond angles of BFBN are presented in Table 1. From the theoretical values, it is found that most of the optimized bond lengths are slightly larger than the experimental values, due to that the theoretical calculations belong to isolated molecule in gaseous phase while the experimental results belong to molecule in solid state[10]. The calculated geometrical parameters represent a good approximation and they are the bases for calculating other parameters, such as vibrational frequencies and thermodynamics properties. The global minimum energy obtained by the DFT

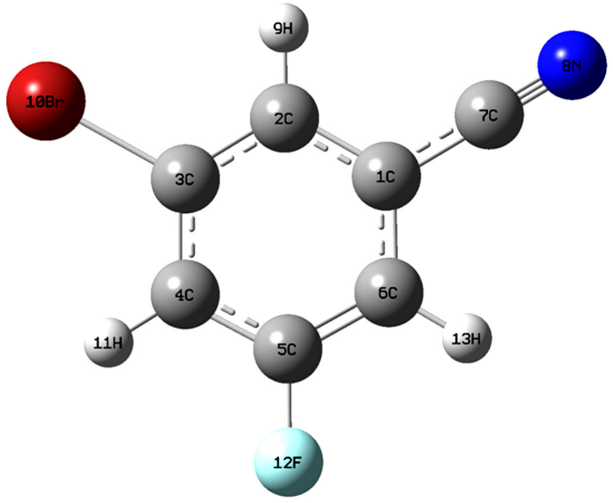

Fig. 1 — Molecular model of 3-bromo-5-flurobenzonitrile along with numbering of atoms.

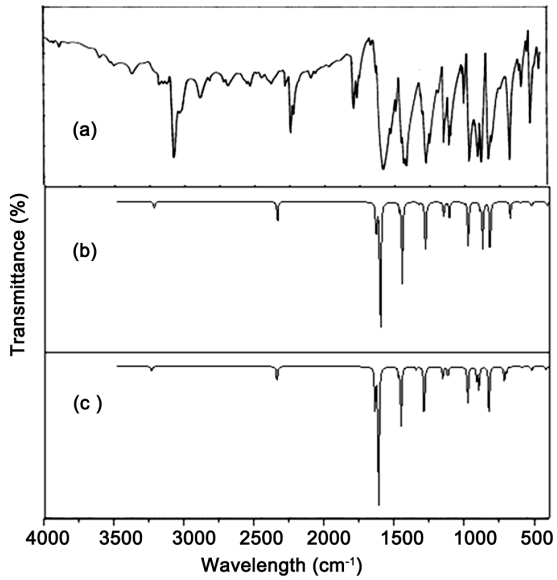

Fig. 2 — Comparison of observed and calculated IR spectra of 3-bromo-5-flurobenzonitrile (a) observed, (b) calculated with B3LYP/6-311++G(d,p) and (c) calculated with B3LYP/6-31+G(d,p).

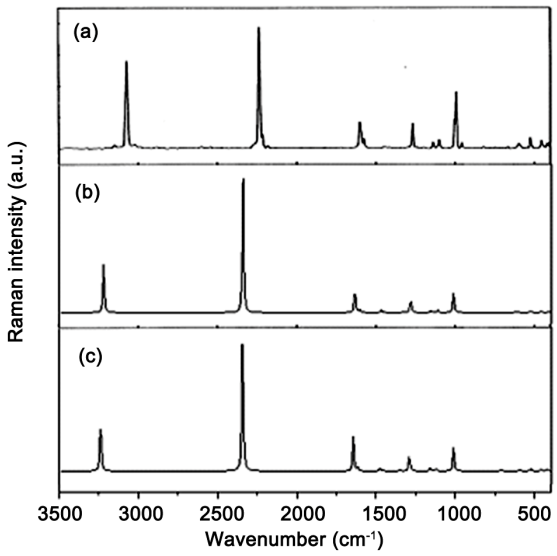

Fig. 3 — Comparison of observed and calculated Raman spectra of 3-bromo-5-flurobenzonitrile (a) observed, (b) calculated with B3LYP/6-311++G(d,p) and (c) calculated with B3LYP/6-31+G(d,p).

structure optimization with the 6-31+G(d,p) and 6-311++G(d,p) basis sets for BFBN are calculated as -2994.87448480 and -2997.38313199 Hartrees, respectively.

Table 1 — Optimized geometrical parameters for 3-bromo-5-fluorobenzonitrile computed at B3LYP/6-31+G(d,p) and 6-311++G(d,p) basis sets.

Parameters	Method/Basis set B3LYP/ 6-31+G(d,p)	B3LYP/ 6-311++G(d,p)	Experimental[a]
Bond length (Å)			
C1-C2	1.404	1.402	1.412
C2-C3	1.393	1.390	1.373
C3-C4	1.395	1.392	1.366
C4-C5	1.390	1.388	1.371
C5-C6	1.387	1.384	1.384
C1-C6	1.404	1.401	1.398
C1-C7	1.435	1.432	1.430
C7-N8	1.163	1.155	1.140
C2-H9	1.082	1.081	0.950
C3-Br10	1.897	1.909	1.884
C4-H11	1.083	1.081	0.950
C5-F12	1.352	1.349	1.355
C6-H13	1.083	1.082	0.950
Bond angle (°)			
C1-C2-C3	118.73	118.75	117.4
C2-C3-C4	121.56	121.61	121.9
C3-C4-C5	117.87	117.84	117.7
C4-C5-C6	123.01	122.94	124.2
C5-C6-C1	117.73	117.86	117.7
C6-C1-C2	121.07	120.96	117.5
C1-C7-N8	180.15	179.98	176.5
C6-C1-C7	119.47	119.57	121.5
C2-C1-C7	119.44	119.46	121.0
C1-C2-H9	120.32	120.27	121.1
C3-C2-H9	120.94	120.97	121.1
C4-C3-Br10	119.11	119.07	119.7
C2-C3-Br10	119.32	119.31	118.4
C5-C4-H11	120.19	120.11	121.3
C3-C4-H11	121.93	122.04	121.3
C6-C5-F12	118.66	118.72	118.5
C4-C5-F12	118.31	118..34	117.3
C1-C6-H13	121.64	121.60	121.3
C5-C6-H13	120.62	120.50	121.3
Dihedral angle (°)			
C6-C1-C2-H9	180.0	179.99	
C7-C1-C2-C3	180.0	179.99	
C2-C1-C6-H13	180.0	-179.99	
C7-C1-C6-C5	180.0	-179.99	
C6-C1-C7-N8	180.0	180.0	
C1-C2-C3-Br10	180.0	-179.99	
H9-C2-C3-C4	180.0	180.00	
C2-C3-C4-H11	180.0	180.00	
Br10-C3-C4-C5	180.0	-180.00	
C3-C4-C5-F12	180.0	180.00	
H11-C4-C5-C6	180.0	-180.00	
C4-C5-C6-H13	180.0	-180.00	
F12-C5-C6-C1	180.0	179.99	

[a]Experimental values are taken from Ref.[11].

The benzene ring appears little distorted and angles slightly out of perfect hexagonal structure. It is due to the substitutions of the fluorine, bromine atoms and C-N group in the place of H atoms. According to the experimental values of similar molecule[11], the order of the optimized bond length of the six C–C bonds of the ring are as C3–C4 < C4–C5 < C2–C3 < C5–C6 < C1–C6 < C1–C2. But, as per the calculated values (B3LYP/6-311++G (d,p)), the order of the bond lengths is slightly differed as C5–C6 < C4–C5 < C2–C3 < C3–C4 < C1–C6 < C1–C2, since the substitutions are different. The benzene ring appears to be distorted with C1–C2 and C1–C6 bond lengths exactly at the substitution place 1.402 and 1.401 Å, respectively, longer than remaining bonds (~1.384 Å to ~1.392 Å cal.) in the ring. The C–F and C–Br bond lengths indicate a considerable increase when substituted in place of C–H. Fluorine and bromine atoms are in the plane of the benzene ring. The C–F and C-Br bond lengths are found to be 1.349 and 1.909 Å by B3LYP/6-311++G (d, p), which are 0.006 and 0.025 Å smaller and larger than the experimental value (1.355 and 1.884 Å), respectively. The changes in the bond length and breakdown of regular hexagonal symmetry of the phenyl ring are attributed to the changes in charge distribution on the carbon atoms of the phenyl ring on substitution with bromine and fluorine atoms. The C-Br and C-F bond lengths determined theoretically are well agreed with the calculated values of 4-bromobenzonitrile[12] and 2,3,4-trifluorobenzonitrile[13].

The C1–C7 bond length of BFBN is longer, where the cyano group is attached. This is due to the electron withdrawing nature of the group. The longer bond length of C1–C2 and C1–C6 indicates that the cyano group exerts larger attraction on valance electron cloud of the ring resulting easy delocalisation of electrons towards the cyano group and thereby decreases in force constant and increase in bond length. The C-CN bond length of p-cyanobenzoic acid[14] (1.432 Å by B3LYP/6-311++G(d,p)) is in excellent agreement with the longer C1-C7 bond of BFBN (1.432 Å). According to the DFT calculations, the bond angles C2–C1–C6, C2–C3–C4 and C4–C5–C6 are lengthened by 0.96°, 1.61° and 2.94° from 120°, respectively, at the C1, C3 and C5 positions and this asymmetry of the exocyclic angles reveals the repulsion between C-N group, bromine, fluorine atoms and the benzene ring. The asymmetry of the benzene ring is also evident by the order of bond

angles C3–C4–C5 < C5–C6–C1 < C1–C2–C3 < C6–C1–C2 < C2–C3–C4 < C4–C5–C6.

4.2 Vibrational assignment

The BFBN consists of 13 atoms, hence undergoes 33 normal modes of vibrations. In agreement with C_s symmetry, the 33 fundamentals are distributed amongst the symmetry species as:

$$\Gamma_{3N-6} = 23A'(\text{in}-\text{plane}) + 10A''(\text{out}-\text{of}-\text{plane}) \quad \ldots (1)$$

All the fundamental vibrations are active in both Raman scattering and IR absorption. The detailed vibrational assignment of fundamental modes of BFBN along with the calculated IR and Raman frequencies and normal mode descriptions (characterized by TED) are reported in Table 2.

The reliable prediction of vibrational spectra is of considerable use in assigning the normal modes of a molecule. Computational methods can also be used to assign the bands of the spectra. The selection of adequate quantum chemical methods and scaling procedures remarkably reduce the risk in the assignment and can accurately determine the contribution of the different modes in an observed band. DFT calculations have been reported to provide excellent vibrational frequencies of organic molecules if the calculated frequencies are scaled to compensate for the approximate treatment of electron correlations, for basis set deficiencies, and for anharmonicity. However, the introduction of scaling factors is capable of accounting for all these effects. A number of studies have been carried out regarding the calculations of vibrational spectra using B3LYP method with the 6-31+G(d,p) and 6-311++G(d,p) basis sets. As a result, it was found that the experimental vibrational frequencies and IR intensities could be reported very accurately. The scaling factor was applied successfully to the B3LYP method and found to be easily transferable to a number of molecules[15]. Therefore, the calculated wavenumbers were scaled by using scaling factor of 0.9613 for B3LYP method[16]. The analyses for the vibrational modes of BFBN were presented in some detail in order to describe the basis for the assignments.

4.2.1 C-H vibrations

The C-H stretching vibrations of benzene derivatives[17] generally appear in the region 3100-3000 cm^{-1}. In this region, the bands are not affected appreciably by the nature of the substituent. Hence, in the present investigation, the FTIR band found at 3103, 3082, and 3015 cm^{-1} and 3078, 3020 cm^{-1} in Raman for BFBN have been assigned to C-H stretching vibrations and these modes are confirmed by their TED values. The bands due to C-H in-plane bending vibrations, interact somewhat with C-C stretching vibrations, are observed as a number of sharp bands in the region 1300-1000 cm^{-1}. The C-H out-of-plane bending vibrations are strongly coupled vibrations and occur in the region 900-667 cm^{-1}. In this study, the FT-Raman bands observed at 1100, 990, 959 cm^{-1} and infrared bands at 1096, 994 cm^{-1} are assigned to C–H in-plane bending vibrations of BFBN. The out-of-plane bending vibrations of C-H group have also been identified for BFBN and they are presented in Table 2. The theoretically computed values for C-H vibrational modes by B3LYP/6-311++G(d,p) method give excellent agreement with experimental data.

4.2.2 C≡N vibrations

For the aromatic compound which bears a C≡N group attached to the ring, a band of very good intensity has been observed in the region 2220-2240 cm^{-1} and it is being attributed to C≡N stretching vibrations[18]. Further, the n–π conjugation between the cyano nitrogen lone electron pair and the phenyl ring is strong in the ground state. The strong bands obtained at 2242 cm^{-1} in IR, 2241 cm^{-1} in Raman spectra are assigned to C≡N stretching vibration for BFBN and the corresponding force constant contribute 88% to the TED. The in-plane and out-of-plane bending modes of C≡N group are strongly coupled with C-C-C bending modes. They are due to the out-of-plane aromatic ring deformation with in-plane deformation of the C≡N vibration and in-plane bending of the aromatic ring with the C–C≡N bending. In this study, the C≡N in-plane vibration is found at 541 cm^{-1} in FTIR and the out-of-plane C≡N bending mode is calculated with null IR intensity and very weak or almost null Raman activity, in accordance with the no-detection of this mode in the experimental spectra. The calculated band at 208 cm^{-1} is assigned to the out-of-plane deformation of C≡N vibration for the title molecule.

4.2.3 C–F vibrations

In the vibrational spectra of related compounds, the bands due to C-F stretching vibrations[19] may be found over a wide frequency range 1360-1000 cm^{-1} since the vibration is easily affected by adjacent atoms or groups. In the present investigation, the IR and Raman bands observed at 1263 and 1266 cm^{-1} have been assigned to C-F stretching mode of vibration for BFBN, which are further supported by the high

value of TED. Normally, the C–F in-plane bending vibrations are expected in the general range 420-375 cm^{-1} and the band at 268 cm^{-1} to C–F out-of-plane bending vibration[13]. In the present case, the FTIR band at 530 cm^{-1} and the calculated band at 125 cm^{-1} are assigned to C-F in-plane and out-of-plane bending vibrations of BFBN, respectively.

4.2.4 C–Br vibrations

Strong characteristic absorption due to the C–Br stretching vibration is observed with the position of

Table 2 – Vibrational assignments of fundamental modes of 3-bromo-5-fluorobenzonitrile along with calculated IR intensity (km/mol), Raman activity (Å amu^{-1}) and normal mode descriptions (characterized by TED) based on quantum mechanical calculations using DFT method.

S. No.	Species C_s	Observed fundamentals (cm^{-1})		Calculated frequencies (cm^{-1}) B3LYP/6-31+G(d,p)				B3LYP/6-311++G(d,p)				TED(%) among types of internal coordinates
		FTIR	Raman	Unscaled	Scaled	IR intensity	Raman activity	Unscaled	Scaled	IR intensity	Raman activity	
1	A′	3103(w)	-	3239	3114	2.91	86.07	3219	3095	2.98	86.99	υCH(99)
2	A′	3082(vs)	3078(vs)	3238	3112	1.48	61.47	3218	3094	1.88	45.41	υCH(98)
3	A′	3015(w)	3020(vw)	3237	3111	2.44	66.20	3217	3093	2.70	74.47	υCH(95)
4	A′	2242(vs)	2241(s)	2342	2252	21.98	485.26	2340	2249	21.87	482.58	υCN(88)
5	A′	-	1610(ms)	1644	1580	46.86	81.90	1634	1571	48.98	79.92	υCC (86)
6	A′	1586(vs)	1584(w)	1619	1556	167.59	8.58	1605	1543	165.96	8.75	υCC(82)
7	A′	1438(s)	-	1477	1420	8.36	5.93	1469	1413	7.84	5.90	υCC (80)
8	A′	1424(s)	-	1458	1401	75.52	2.53	1449	1393	78.25	2.60	υCC (78)
9	A′	1305(w)	-	1350	1297	3.54	3.16	1332	1281	3.35	2.78	υCC (74)
10	A′	1263(s)	1266(ms)	1292	1242	68.26	40.07	1284	1234	69.68	38.27	υCF(70), βCC (22)
11	A′	1241(s)	-	1274	1225	1.94	1.28	1263	1214	2.39	1.30	υCC (76)
12	A′	1149(ms)	1146(w)	1160	1115	16.60	7.52	1153	1108	18.69	6.57	υCC (78)
13	A′	1096(s)	1100(w)	1124	1080	16.42	6.28	1113	1070	15.99	5.59	βCH(72), βCC(20)
14	A′	994(ms)	990(s)	1013	974	0.63	58.17	1013	973	1.44	57.46	βCH(70), βCC (17)
15	A′	-	959(w)	982	944	48.18	1.63	978	940	50.14	2.01	βCH(72), βCC(20)
16	A′	-	820(vw)	831	799	61.25	0.59	823	791	64.24	0.51	Rtrig(59), βCC (40)
17	A′	677(s)	-	725	695	17.66	0.86	679	653	15.87	0.36	υCBr(64), R_{asym}(16)
18	A′	-	607(ms)	705	678	7.97	1.55	622	598	0.02	2.24	R_{sym}(69), βCC (20)
19	A′	-	595(w)	600	577	0.30	1.25	605	582	1.01	1.80	R_{asym}(68), βCC(18)
20	A′	584(ms)	-	594	571	0.94	1.79	554	533	0.13	0.14	βCCN(71), βCN(20)
21	A′	541(ms)	-	527	507	5.97	5.64	528	508	6.56	5.44	βCN(69), βCC(15),R_{trig}(13)
22	A′	530(s)	-	461	443	0.16	3.97	462	444	0.18	3.79	βCF(68), βCC(15),R_{asym}(12)
23	A′	-	518(ms)	426	409	3.65	2.33	421	405	1.51	1.81	βCBr(69), R_{sym}(23)
24	A′′	950(ms)	-	921	885	5.07	0.07	902	868	0.02	0.12	γCH(66), γCC(18)
25	A′′	874(ms)	-	918	883	13.18	0.10	894	859	9.70	0.08	γCH(65),τR_{sym}(18)
26	A′′	844(ms)	-	902	867	25.12	0.07	875	841	44.47	0.13	γCH(64), τR_{trig}(29)
27	A′′	455(ms)	-	417	401	1.44	2.01	412	396	3.51	1.87	τR_{sym}(62), γCC(24)
28	A′′	-	446(w)	304	293	3.20	4.64	300	288	3.60	4.81	τR_{asym}(61),γCBr (18), γCC(12)
29	A′′	-	417(w)	246	237	0.26	2.18	238	228	0.35	1.86	τR_{trig} (60),γCH(20)
30	A′′	-	408(w)	210	202	0.23	1.24	207	199	1.12	1.37	γCCN(62), τR_{sym} (25)
31	A′′	-	-	208	200	1.13	1.26	177	170	0.93	0.94	γCN(58),γCC(23), τR_{sym}(14)
32	A′′	-	-	125	121	4.38	0.25	121	116	4.04	5.17	γCF(58) τR_{sym}(25)
33	A′′	-	-	119	114	4.21	5.39	118	114	3.74	0.30	γCBr(61),τR_{asym} (28)

Abbreviations used: υ-stretching; β-in-plane bending; γ-out-of-plane bending; R_{sym}-ring symmetric; R_{asym}-ring asymmetric; R_{trig}-ring trigonal; τ-torsion; s-strong; vs-very strong; ms-medium strong; w-weak; vw-very weak.

the band being influenced by neighbouring atoms or groups, the smaller the halide atom, the greater the influence of the neighbour[20]. Bands of weak to medium intensity are also observed for the C–Br stretching vibrations. The C–Br bond shows lower absorption frequencies as compared to C–H bond due to the decreased force constant and increase in reduced mass[12]. According to the early reports[21], the C–Br stretching vibration gives generally strong band in the region 675–560 cm^{-1}. In BFBN, the band is observed at 677 cm^{-1} in IR for C–Br stretching and this assignment is in line with the literature. The corresponding force constant contributes 64% to the TED. The Raman band at 518 cm^{-1} and the calculated band at 119 cm^{-1} have been assigned for C–Br in-plane and out-of-plane bending vibrations for BFBN. The influence of other substitution on C–Br stretching and deformation bands is significant in this compound.

4.2.5 C-C vibrations

The bands between 1400 and 1625 cm^{-1} in benzene derivatives are due to C-C stretching vibrations[22]. Therefore, the C-C stretching vibrations of BFBN are found at 1586, 1438, 1424, 1305, 1241 and 1149 cm^{-1} in the FTIR and at 1610, 1584, 1146 cm^{-1} in the FT-Raman spectrum and these modes are confirmed by their TED values. Most of the ring vibrational modes are affected by the substitutions in the aromatic ring of BFBN. The C-C-C in-plane bending bands[23] always occur between the range 1000–600 cm^{-1}. In the present study, the bands observed at 820, 607 and 595 cm^{-1} in the Raman spectrum have been designated to ring in-plane bending modes by careful consideration of their quantitative descriptions. The higher percentage of TED obtained for this group encouraging and confirms the assignments proposed in this study for ring in-plane bending vibrations of BFBN. The ring out-of-plane bending modes of BFBN are also listed in the Table 2.

4.3 Vibrational contribution to NLO activity and first hyperpolarizability

Linear and non-linear optical properties of molecular crystals have attracted considerable attention for both practical and theoretical reasons. The potential application of the title compound in the field of nonlinear optics demands the investigation of its structural and bonding features contributing to the hyperpolarizability enhancement, by analyzing the vibrational modes using IR and Raman spectroscopy. The first hyperpolarizability (β) of this molecular system is calculated using B3LYP/6-311++G(d,p) method, based on the finite field approach. In the presence of an applied electric field, the energy of a system is a function of the electric field. The first hyperpolarizability is a third-rank tensor that can be described by a 3×3×3 matrix. The 27 components of the 3D matrix can be reduced to 10 components due to the Kleinman symmetry[24].

The components of β are defined as the coefficients in the Taylor series expansion of the energy in the external electric field. When the electric field is weak and homogeneous, this expansion becomes:

$$E = E_0 - \sum_i \mu_i F^i - \frac{1}{2}\sum_{ij} \alpha_{ij} F^i F^j - \frac{1}{6}\sum_{ijk} \beta_{ijk} F^i F^j F^k - \frac{1}{24}\sum_{ijkl} \nu_{ijkl} F^i F^j F^k F^l + \ldots \quad \ldots (2)$$

where E_0 is the energy of the unperturbed molecule; F^i is the field at the origin; and μ_i , α_{ij}, β_{ijk} and ν_{ijkl} are the components of dipole moment, polarizability, the first hyperpolarizabilities and second hyperpolarizibilites, respectively. The total static dipole moment μ, the mean polarizability α_0 and the mean first hyperpolarizability β_0, using the *x*, *y*, *z* components are defined as follows:

$$\mu = (\mu_x^2 + \mu_y^2 + \mu_z^2)^{1/2} \quad \ldots (3)$$

$$\bar{\alpha} = \frac{1}{3}(\alpha_{xx} + \alpha_{yy} + \alpha_{zz}) \quad \ldots (4)$$

$$\Delta\alpha = \frac{1}{\sqrt{2}}\left[\begin{array}{l}(\alpha_{xx} - \alpha_{yy})^2 + (\alpha_{yy} - \alpha_{zz})^2 \\ +(\alpha_{zz} - \alpha_{xx})^2 + 6\alpha_{xx}^2\end{array}\right]^{1/2} \quad \ldots (5)$$

$$\beta = \left[\begin{array}{l}\left(\beta_{xxx} + \beta_{xyy} + \beta_{xzz}\right)^2 \\ +\left(\beta_{yyy} + \beta_{xxy} + \beta_{yzz}\right)^2 \\ +\left(\beta_{zzz} + \beta_{xxz} + \beta_{yyz}\right)^2\end{array}\right]^{1/2} \quad \ldots (6)$$

The components of dipole moment, polarizability and the first hyperpolarizability of the title compound can be seen in Table 3. The calculated values of total static dipole moment μ, the average linear polarizability $\bar{\alpha}$, the anisotropy of the polarizability Δα, and the first hyperpolarizability β using the DFT-B3LYP/6-311++G(d,p) method are 2.9425 Debye, 15.6195 $Å^3$, 31.4392 $Å^3$ and 1.585×10^{-30} cm^5 $e.s.u.^{-1}$,

respectively, which are comparable with the reported values of similar derivatives[25]. Urea is one of the prototypical molecules used in the study of the NLO properties of molecular systems and frequently used as a threshold value for comparative purposes. The values of μ, $\bar{\alpha}$ and β obtained by Sun *et al.*[26] with the B3LYP/6-311++G(d,p) method for urea are 1.373 Debye, 3.831 Å^3 and 3.729×10^{-31} cm^5 e.s.u.$^{-1}$, respectively. The first hyperpolarizability of the title compound is 4 times greater than that of urea. According to the magnitude of the first hyperpolarizability, the title compound may be a potential applicant in the development of NLO materials. Thus, this molecule might serve as a prospective building block for nonlinear optical materials.

4.4 Thermodynamic properties

On the basis of vibrational analysis at B3LYP/6-311++G(d,p) level, the standard statistical thermodynamic functions; heat capacity (*C*), entropy (*S*), and enthalpy changes (Δ*H*), for the title compound have been obtained from the theoretical harmonic frequencies and are listed in Table 4. From Table 4, it can be observed that all these thermodynamic functions are increasing with temperature ranging from 100 to 600 K due to the fact that the molecular vibrational intensities increase with temperature[27]. All the thermodynamic data supply helpful information for the further study on the BFBN. They can be used to compute other thermodynamic energies according to relationships of thermodynamic functions and estimate directions of chemical reactions according to the second law of thermodynamics in thermochemical field[28].

Table 3 — Calculated dipole moment μ (Debye), polarizability (α) and the first hyperpolarizability (β) components (a.u.) for 3-bromo-5-fluorobenzonitrile.

Components	Values	Components	Values
μ_x	1.7534	β_{xxx}	-158.7705
μ_y	2.3630	β_{xxy}	17.3189
μ_z	0.0000	β_{xyy}	59.3630
		β_{yyy}	-204.8999
α_{xx}	113.6391	β_{xxz}	0.0003
α_{xy}	8.8619	β_{xyz}	0.0002
α_{yy}	146.9761	β_{yyz}	0.0001
α_{xz}	0.0001	β_{xzz}	-5.7842
α_{yz}	0.0003	β_{yzz}	37.3101
α_{zz}	55.9315	β_{zzz}	0.0001

Table 4 — Thermodynamic properties at different temperatures at the B3LYP/6-311++G(d,p) level for 3-bromo-5 fluorobenzonitrile.

T (K)	*C* (J/mol.K)	*S* (J/mol.K)	Δ*H* (kJ/mol)
100.00	285.95	63.65	4.45
200.00	341.94	101.85	12.75
298.15	389.13	136.09	24.46
300.00	389.97	136.69	24.71
400.00	433.49	166.31	39.91
500.00	473.26	190.06	57.77
600.00	509.63	208.70	77.75

4.5 UV-Vis and HOMO-LUMO analysis

The frontier molecular orbitals (FMOs) play an important role in the electric and optical properties, as well as in UV–Vis spectra and chemical reactions[29]. In order to evaluate the energetic behaviour of the title compound, calculations in DMSO, water, ethanol and gas phase have been carried out by using TD-DFT/B3LYP/6-311++G(d,p). The calculated absorption wavelengths (λ), oscillator strengths (*f*) and excitation energies (*E*) are given Table 5. The theoretical ultraviolet spectrum of BFBN in gas and solvent phase is shown in Fig. 4. According to the Frank–Condon principle, the maximum absorption peak (λ_{max}) in an UV–visible spectrum corresponds to vertical excitation. The TD-DFT calculations predict three transitions in the UV–Vis region for BFBN molecule. The strong transitions at 4.6447 eV (266.94 nm) with an oscillator strength f = 0.0368 in gas phase, at 4.5857 eV (270.37 nm) with an oscillator strength f = 0.0582 and at 4.5883 eV (270.22 nm) with an oscillator strength f = 0.0550 in DMSO and water, respectively, are assigned to a $\pi \rightarrow \pi^*$ transition. For ethanol solvent, the strong transitions are found at 4.5889 eV (270.18 nm) with an oscillator strength f = 0.0560. The major contributions of the transitions were designated with the aid of SWizard program[30]. In view of calculated absorption spectra, the maximum absorption wavelength corresponds to the electronic transition from the highest occupied molecular orbital HOMO to lowest unoccupied molecular orbital LUMO with 85% contribution and is assigned to $\pi \rightarrow \pi^*$ transition. The absorption wavelength corresponding to the electronic transition from HOMO to LUMO+2 (97%) and from HOMO-2 to LUMO (98%) are assigned to $\pi \rightarrow \pi^*$ type.

This electronic absorption corresponds to the transition from the ground to the first excited state and is mainly described by one electron excitation from the highest occupied molecular orbital (HOMO) to the lowest unoccupied molecular orbital[31] (LUMO). The LUMO as an electron acceptor (EA) represents the

Table 5 — The calculated absorption wavelength λ (nm), excitation energies *E* (eV) and oscillator strengths (*f*) of BFBN calculated by the TD-B3LYP/6-311++G(d,p) method in gas and solvent phase

TD-B3LYP/6-311++G(d,p)												Major contribution	Assignment
DMSO			Water			Ethanol			Gas				
λ (nm)	*E* (eV)	*f*	λ (nm)	*E* (eV)	*f*	λ (nm)	*E* (eV)	*f*	λ (nm)	*E* (eV)	*f*		
270.37	4.5857	0.0582	270.22	4.5883	0.0550	270.18	4.5889	0.0560	266.94	4.6447	0.0368	H → L (85%)	π → π*
228.16	5.4342	0.0002	228.10	5.4355	0.0002	228.14	5.4346	0.0002	228.63	5.4228	0.0001	H → L+2 (97%)	π → π*
226.15	5.4825	0.0001	226.14	5.4825	0.0001	226.13	5.4828	0.0001	225.21	5.5053	0.0001	H-2 → L (98%)	π → π*

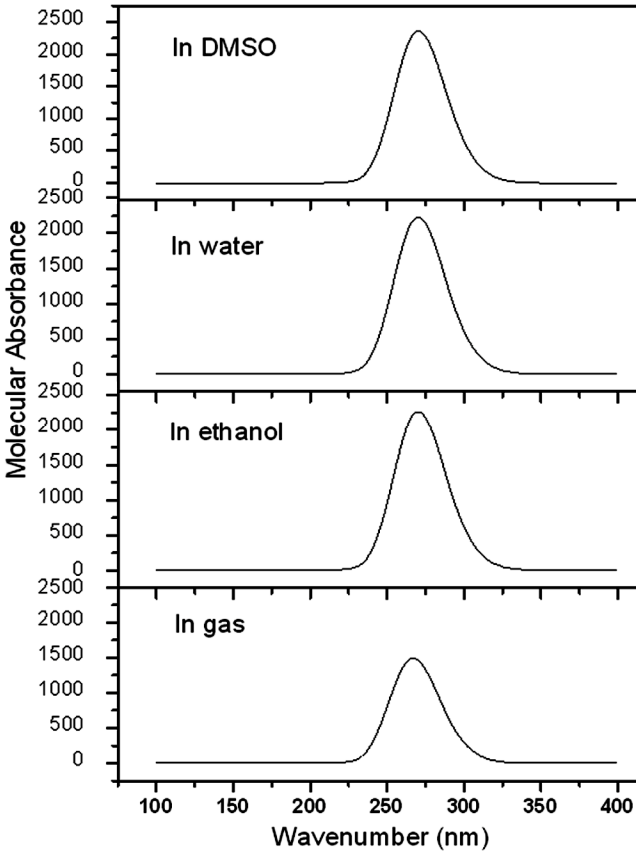

Fig. 4 — Theoretically calculated UV spectra in gas and solvent phase for 3-bromo-5-flurobenzonitrile.

ability to obtain an electron and HOMO represents ability to donate an electron (ED). The electron transfer from ED groups to the efficient EA groups takes place through π-conjugated path. The energies of four important molecular orbitals of BFBN; the second highest and highest occupied MO's (HOMO and HOMO-1), the lowest and the second lowest unoccupied MO's (LUMO and LUMO+1) have been calculated using TD-B3LYP/6- 311++G(d,p) and are presented in Table 6. The 3D plots of the HOMO-1, HOMO, LUMO and LUMO+1 orbitals computed at the B3LYP/6-311G++(d,p) level for BFBN (in gas phase) are illustrated in Fig. 5. In BFBN, the HOMO

Table 6 — Calculated HOMO-LUMO energy values of 3-bromo-5-fluorobenzonitrile calculated in gas and solvent phase.

Parameters	TD-B3LYP/6-311++G(d,p)			
	DMSO	Water	Ethanol	Gas
E_{HOMO} energy (eV)	-7.469	-7.466	-7.476	-7.738
E_{LUMO} energy (eV)	-2.210	-2.207	-2.215	-2.416
$\Delta E_{HOMO\text{-}LUMO\ energy\ gap}$ (eV)	5.259	5.259	5.261	5.322
$E_{HOMO\text{-}1}$ energy (eV)	-7.849	-7.847	-7.855	-8.074
E_{LUMO+1} energy (eV)	-1.291	-1.287	-1.299	-1.593
$\Delta E_{HOMO\text{-}1\text{-}LUMO+1energy\ gap}$ (eV)	6.558	6.560	6.556	6.481
Electronegativity χ (eV)	4.839	4.836	4.845	5.077
Chemical hardness η (eV)	2.629	2.629	2.630	2.661
Softness ξ $(eV)^{-1}$	0.380	0.380	0.380	0.376
Electrophilicity index ψ (eV)	4.453	4.448	4.463	4.843
Dipole moment (Debye)	3.773	3.785	3.750	2.942

is located over C≡N group, fluorine and bromine atoms and LUMO of π nature, (i.e., benzene ring) is delocalized over the whole C-C bond; consequently the HOMO→LUMO transition implies an electron density transfer to the C–C bond of the benzene ring from fluorine and bromine atoms. Moreover, these orbital significantly overlap in their position for BFBN. The energy gap of HOMO–LUMO explains the eventual charge transfer interaction within the molecule, which influences the biological activity of the molecule. Furthermore, in going from the gas phase to the solvent phase, there is a decreasing value of the energy gap and molecule becomes more stable. The frontier orbital gap in case of BFBN is found to be 5.259, 5.259, 5.261, 5.322 eV for DMSO, water, ethanol and gas phase, respectively, as shown in Table 6. The decrease in energy gap between HOMO and LUMO facilitates intra molecular charge transfer which makes the material to be NLO active.

The electronic properties of the molecule are calculated from the total energies and the Koopmans' theorem. The ionization potential is determined from

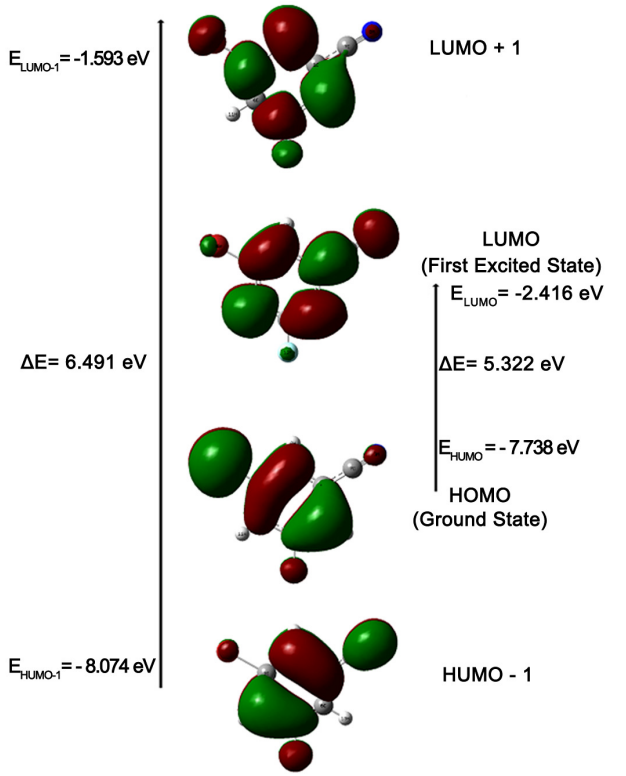

Fig. 5 — Atomic orbital compositions of the frontier molecular orbital for 3-bromo-5-flurobenzonitrile.

the energy difference between the energy of the compound derived from electron-transfer (radical cation) and the respective neutral compound; IP = $E_{cation} - E_n = -E_{HOMO}$ while the electron affinity is computed from the energy difference between the neutral molecule and the anion molecule: EA = $E_n - E_{anion} = -E_{LUMO}$, respectively. The other important quantities such as electronegativity (χ), hardness (η), softness (ξ), and electrophilicity index (ψ) were deduced from ionization potential and electron affinity values[32]:

$$(\chi)\mu \approx -\chi = \frac{IP + EA}{2} \quad \ldots (7)$$

$$(\eta) \approx \frac{IP - EA}{2} \quad \ldots (8)$$

$$(\xi) \approx \frac{1}{\eta} \quad \ldots (9)$$

$$(\psi) \approx \frac{\mu^2}{2\eta} \quad \ldots (10)$$

The values of electro negativity, chemical hardness, softness, and electrophilicity index of BFBN are 4.836, 2.629, 0.380 and 4.448 eV in water, respectively. According to maximum hardness principle (MHP), the most stable structure should have maximum hardness value which being a minimum energy structure at constant chemical potential and hence the principle of maximum hardness has been proved in the present study.

4.6 NBO analysis

Natural bond orbital (NBO) analysis is one of the most powerful tools for interpreting quantum-chemical results in terms of chemically significant terms. This method localizes the molecular wave functions in optimized electron pairs, corresponding to lone pairs; core pairs on bonding units; giving a picture which is close to the familiar Lewis picture of molecular structure. In the present study, the NBO calculations were performed on BFBN using NBO 3.1 program as implemented in the Gaussian 09 package at the DFT/B3LYP level in order to understand various second-order interactions between the filled orbitals of one subsystem and vacant orbitals of another subsystem, which is the measure of the delocalization or hyperconjugation. By the use of the second-order bond–antibond (donor–acceptor) NBO energetic analysis, insight in the most important delocalization schemes was obtained. The change in electron density (ED) of (σ*, π*) antibonding orbitals and $E(2)$ energies have been calculated by NBO analysis using DFT method to give clear evidence of stabilization originating from various molecular interactions. The hyperconjugative interaction energy was deduced from the second-order perturbation approach[33]. For each donor (i) and acceptor (j), the stabilization energy E_2 associated with the delocalization $i \rightarrow j$ is estimated as:

$$E_2 = \Delta E_{ij} = q_i \frac{F(i,j)^2}{\varepsilon_i - \varepsilon_j} \quad \ldots (11)$$

where q_i is the donor orbital occupancy, ε_i and ε_j are diagonal elements and $F(i,j)$ is the off diagonal NBO Fock matrix element. The intra-molecular charge transfer is one of the strongest causes for NLO activity. The second order perturbation theory analysis of Fock matrix in NBO basis of BFBN (Table 7) indicates the intra-molecular interactions due to the orbital overlap of $\pi(C_1\text{-}C_2)$ with $\pi^*(C_3\text{-}C_4)$, resulting in high electron density (approximately 0.195 e) of anti-bonding π orbitals (C-C) which causes stabilization of 10.46 kcal/mol to the system. Similarly, the charge transfer from $\pi(C_3 - C_4)$ to $\pi^*(C_5 - C_6)$ amounts to the stabilization of 10.23

Table 7 — Second-order perturbation theory analysis of Fock matrix in NBO basis for BFBN.

Donor (*i*)	ED (*i*) (e)	Acceptor (*j*)	ED (*j*) (e)	[a]*E*(2) (kJ mol^{-1})	[b]*E*(*j*)–*E*(*i*) (a.u.)	[c]*F* (*i*,*j*) (a.u.)
$\sigma(C_1 - C_2)$	0.97997	$\sigma^*(C_1 - C_6)$	0.01134	1.98	1.26	0.063
		$\sigma^*(C_3 - Br_{10})$	0.01567	2.61	0.80	0.058
		$\sigma^*(C_7 - N_8)$	0.00525	2.10	1.64	0.075
$\pi(C_1 - C_2)$	0.82622	$\pi^*(C_3 - C_4)$	0.19466	10.46	0.27	0.068
		$\pi^*(C_5 - C_6)$	0.17529	9.63	0.28	0.065
$\sigma(C_1 - C_6)$	0.98196	$\sigma^*(C_1 - C_2)$	0.01307	2.04	1.26	0.064
		$\sigma^*(C_5 - F_{12})$	0.01472	2.06	0.98	0.057
		$\sigma^*(C_7 - N_8)$	0.00525	2.11	1.64	0.075
$\sigma(C_1 - C_7)$	0.98924	$\sigma^*(C_1 - C_2)$	0.01307	1.22	1.27	0.050
		$\sigma^*(C_7 - N_8)$	0.00525	4.04	1.65	0.103
$\sigma(C_2 - C_3)$	0.98975	$\sigma^*(C_1 - C_2)$	0.01307	1.57	1.29	0.057
$\sigma(C_2 - H_9)$	0.98856	$\sigma^*(C_1 - C_6)$	0.01134	2.06	1.08	0.059
		$\sigma^*(C_3 - C_4)$	0.01238	2.21	1.08	0.062
$\sigma(C_3 - C_4)$	0.98827	$\sigma^*(C_2 - C_3)$	0.01209	1.54	1.30	0.057
		$\sigma^*(C_5 - F_{12})$	0.01472	1.72	1.00	0.053
$\pi(C_3 - C_4)$	0.83780	$\pi^*(C_1 - C_2)$	0.19447	9.74	0.29	0.069
		$\pi^*(C_5 - C_6)$	0.17529	10.23	0.29	0.069
$\sigma(C_3 - Br_{10})$	0.99170	$\sigma^*(C_1 - C_2)$	0.01307	1.49	1.20	0.053
		$\sigma^*(C_4 - C_5)$	0.01424	1.23	1.19	0.048
$\sigma(C_4 - C_5)$	0.98636	$\sigma^*(C_3 - Br_{10})$	0.01567	2.63	0.82	0.059
		$\sigma^*(C_5 - C_6)$	0.01255	1.98	1.28	0.064
$\sigma(C_4 - H_{11})$	0.98752	$\sigma^*(C_2 - C_3)$	0.01209	2.11	1.10	0.061
		$\sigma^*(C_5 - C_6)$	0.01255	1.83	1.09	0.056
$\sigma(C_5 - C_6)$	0.98987	$\sigma^*(C_1 - C_7)$	0.01529	1.60	1.24	0.056
		$\sigma^*(C_4 - C_5)$	0.01424	1.98	1.28	0.064
$\pi(C_5 - C_6)$	0.82272	$\pi^*(C_1 - C_2)$	0.19447	10.39	0.29	0.070
		$\pi^*(C_3 - C_4)$	0.19466	10.26	0.28	0.068
$\sigma(C_6 - H_{13})$	0.98823	$\sigma^*(C_1 - C_2)$	0.01307	2.03	1.08	0.059
		$\sigma^*(C_4 - C_5)$	0.01424	1.92	1.08	0.058
$\sigma(C_7 - N_8)$	0.99719	$\sigma^*(C_1 - C_7)$	0.01529	3.60	1.54	0.095
$\pi(C_7 - N_8)$	0.99375	$\sigma^*(C_1 - C_2)$	0.01307	1.44	0.88	0.045
		$\sigma^*(C_1 - C_6)$	0.01134	1.45	0.88	0.045
$n1(N_8)$	0.98590	$\sigma^*(C_1 - C_7)$	0.01529	5.73	1.01	0.096
$n1(Br_{10})$	0.99657	$\sigma^*(C_2 - C_3)$	0.01209	0.79	1.55	0.044
		$\sigma^*(C_3 - C_4)$	0.01238	0.78	1.54	0.044
$n2(Br_{10})$	0.98724	$\sigma^*(C_2 - C_3)$	0.01209	1.65	0.85	0.047
		$\sigma^*(C_3 - C_4)$	0.01238	1.74	0.84	0.048
$n3(Br_{10})$	0.96451	$\pi^*(C_3 - C_4)$	0.19466	5.38	0.29	0.054
$n2(F_{12})$	0.98538	$\sigma^*(C_4 - C_5)$	0.01424	3.12	0.96	0.069
		$\sigma^*(C_5 - C_6)$	0.01255	2.99	0.97	0.068
$n3(F_{12})$	0.96128	$\pi^*(C_5 - C_6)$	0.17529	9.46	0.43	0.086
$\pi^*(C_3 - C_4)$	0.19466	$\pi^*(C_1 - C_2)$	0.19447	148.49	0.01	0.082

kcal/mol and the charge transfer from $\pi(C_5 - C_6)$ to $\pi^*(C_1 - C_2)$ amounts to the stabilization of 10.39 kcal/mol. Further, the magnitude of charge transfer from the lone pairs of N8 to anti-bonding C1–C7, σ orbital amount to the stabilization of 5.73 kcal/mol, while the lone pairs of fluorine $n3(F_{12}) \rightarrow \pi^*(C_5 - C_6)$ and bromine $n3(Br_{10}) \rightarrow \pi^*(C_3 - C_4)$, it is of the order of 9.46 and 5.38 kcal/mol, respectively. This interaction is responsible for a pronounced decrease of the lone pair orbital occupancy (approximately 0.96 e) than the other occupancy, and there is a possibility for hyper conjugation between fluorine, bromine atoms and the benzene ring.

5 Conclusions

Based on the scaled quantum mechanical force field obtained by DFT/B3LYP method with 6-31+G(d,p) and 6-311++G(d,p) basis sets, complete vibrational properties of 3-bromo-5-fluorobenzonitrile have been investigated by FTIR and FT-Raman spectroscopy. The various modes of vibrations were unambiguously assigned based on the results of the TED output. The results confirm the ability of the methodology applied for interpretation of the vibrational spectra of the title compound in solid phase. The HOMO and LUMO energy gap explains the eventual charge transfer interactions taking place

within the molecule. NBO results reflect the charge transfer mainly due to the lone pair n1(N_8) → σ^*(C – C), n3(Br_{10}) → π^*(C – C) and n3(F_{12}) → π^*(C – C). To evaluate the electronic transitions and charge distribution, the UV spectra of title compound were calculated. Theoretical molecular orbital coefficient analysis suggests that electronic transitions are assigned to $\pi \rightarrow \pi^*$ type. From the thermodynamic properties, it is seen that the heat capacities, entropies and enthalpies increase with the increasing temperature owing to the intensities of the molecular vibrations increase with increasing temperature. Furthermore, the polarizability, the first hyperpolarizability and total dipole moment of title molecule have been calculated and the results have been discussed. These results indicate that the BFBN compound is a good candidate of nonlinear optical materials.

References

1 Parasad P N & Williams D J, *Introduction to nonlinear optical effects in molecules and polymers*, (John Wiley & Sons: New York), 1991.
2 Rastogi V K, Palafox M A, Tomar R & Singh U, *Spectrochim Acta*, 110A (2013) 458.
3 Agarwal P, Bee S, Gupta A, Tandon P, Rastogi V K, Mishra S & Rawat P, *Spectrochim Acta*, 121A (2014) 464.
4 Palafox M A, Bhat D, Goyal Y, Ahmad S, Joe I H & Rastogi V K, *Spectrochim Acta*, 136A (2015) 464.
5 Zhengyu Z, Dongmei Du, Aiping Fu & Qingsen Yu, *J Mol Struct*, 530 (2000) 149.
6 Frisch M J, Trucks G W & Schlegal H B, *Gaussian 09*, (Gaussian, Inc: Wallingford CT), 2009.
7 Becke A D, *J Chem Phys*, 98 (1993) 5648.
8 Lee C, Yang W & Parr R G, *Phys Rev*, 37 (1998) 785.
9 MOLVIB (v.7.0) *Calculation of hormonic force fields and vibrational modes of molecules*, QCPE program No.807, 2002.
10 Mariappan G & Sundaraganesan N, *J Mol Struct*, 1063 (2014) 192.
11 Britton D, Noland W E & Henke T K, *Acta Cryst*, 58 (2002) 185.
12 Krishnakumar V, Surumbarkuzhali N & Muthunatesan S, *Spectrochim Acta*, 71 (2009) 1810.
13 Hiremath C S, Kalkoti G B & Aralakkanavar M K, *Spectrochim Acta,* 74A (2009) 200.
14 Arjunan V, Rani T, Varalakshmy L, Mohan S & Tedlamelekot F, *Spectrochim Acta*, 78A (2011) 1449.
15 Misra N, Prasad O, Sinha L & Pandey A, *J Mol Struct Theochem*, 822 (2007) 45.
16 Young D C, *Computional chemistry: A practical guide for applying techniques to real-world problems*, (John Wiley & Sons, Inc: New York), 2001.
17 Jeyavijayan S, *J Mol Struct*, 1085 (2015) 137.
18 Nataraj A, Balachandran V & Karthick T, *J Mol Struct*, 1038 (2013) 134.
19 Arivazhagan M, Meenakshi R & Prabhakaran S, *Spectrochim Acta*, 102A (2013) 59.
20 Ramalingam S, Periandy S, Narayanan B & Mohan S, *Spectrochim Acta*, 76A (2010) 84.
21 Carthigayan K, Arjunan V, Anitha R, Periandy S & Mohan S, *J Mol Struct*,1056 (2014) 38.
22 Gnanasambandan T, Gunasekaran S & Seshadri S, *J Mol Struct*, 1052 (2013) 38.
23 Govindarasu K & Kavitha E, *J Mol Struct*, 1088 (2015) 70.
24 Karpagam J, Sundaraganesan N, Sebastian S, Manoharan S & Kurt M, *J Raman Spectorsc*, 41(2010) 53.
25 Senthil K J, Jeyavijayan S & Arivazhagan M, *Spectrochim Acta*, 136A (2015) 234.
26 Sun Y X, Hao Q L, Wei W X, Yu Z X, Lu L D, Wang X & Wang Y S, *J Mol Struct*, 904 (2009) 74.
27 Bevan O J & Boerio-Goates J, *Calculations from statistical thermodynamics*, (Academic Press), 2000.
28 Zhang R, Dub B, Sun G & Sun Y, *Spectrochim Acta*, 75A (2010) 1115.
29 Prabhaharan M, Prabakaran A R, Srinivasan S & Gunasekaran S, *Spectrochim Acta*, 138A (2015) 711.
30 Gorelsky S I, *SWizard program revision 4.5*, University of Ottawa, Ottawa, Canada, 2010, http://www.sg.chem.net/.
31 Kavitha E, Sundaraganesan N & Sebastin S, *Indian J Pure Appl Phys*, 48 (2010) 20.
32 Joseph L, Sajan D, Chaitanya K & Isac J, *Spectrochim Acta*, 122A (2014) 375.
33 Glendening E D, Badenhoop J K, Reed A E, Carpenter J E, Bohmann J A, Morales C M & Weinhold F, *NBO 5.0, Theoretical Chemistry Institute,* University of Wisconsin, Madison, (2001).